**Aalto University**
**MS-E2107 Independent Research Projects in Systems and Operations Research**

# On the Effects of Ground Motion Incoherence on a Nuclear Power Plant

Eeli Asikainen

Espoo: June 18, 2025

# Preface

This project was provided and funded by Fortum Power and Heat Oy. I am sincerely grateful for the opportunity to work on this project and for the supportive environment and excellent collaboration Fortum has offered throughout.

I would especially like to thank my outstanding advisors—Jukka Koskenranta, Joonas Koskinen, Timo Leppänen, and Olli Suurnäkki—for their valuable guidance and help in navigating the topic and identifying relevant materials. I am also thankful to Juhana Vehmas and Sami Sirén for their assistance with the initial practicalities related to the project.

And finally, many thanks to my supervisor, Ahti Salo, for the clear instructions and constructive feedback.

Espoo: June 18, 2025

Eeli Asikainen

# Contents

**Symbols and Abbreviations** **4**

**1 Introduction** **5**

**2 Background** **6**
2.1 Safety Assessment of Nuclear Power Plants . . . . . 6
2.2 Response Spectra . . . . . 7
2.3 Soil-Structure Interaction . . . . . 8

**3 Ground Motion Incoherence** **9**
3.1 Coherency Function . . . . . 9
3.1.1 Mathematical Formulation . . . . . 9
3.1.2 Empirical Coherency Models . . . . . 10
3.2 Impact of Soil and Rock Characteristics . . . . . 11
3.3 Modeling of GMI . . . . . 12
3.3.1 Direct Application of GMI in SSI Analysis . . . . . 12
3.3.2 Scaling Input Fourier Amplitude . . . . . 13
3.3.3 Base Slab Averaging . . . . . 14
3.3.4 Response Spectra Reduction Factors . . . . . 15
3.4 GMI in Prior Research . . . . . 17

**4 Discussion and Computational Example** **19**
4.1 Recommendation for the Modeling of GMI for Loviisa NPP . . . . . 19
4.2 Computational Example of the Use of Reduction Factors . . . . . 20

**5 Conclusion** **22**

**References** **23**

# Symbols and Abbreviations

## Symbols

| | |
|---|---|
| $\omega$ | Ground motion frequency (Hz) |
| $\gamma_{ij}(\omega)$ | Coherency function between stations $i$ and $j$ at frequency $\omega$ |
| $S_{ij}(\omega)$ | Smoothed cross-spectral density between stations $i$ and $j$ |
| $S_{ii}(\omega)$ | Auto-spectral density of station $i$ |
| $d_{ij}$ | Separation distance between $i$ and $j$ (m) |
| $\bar{v}_s$ | Average shear wave velocity (m/s) |
| $RRSB_{sa}$ | Modification factor in base slab averaging |
| $b_e$ | Effective foundation size (m) |
| $T$ | Spectral period of interest (s) |
| $d$ | Foundation plan dimension |
| $r(\omega, d)$ | Spectral reduction factor at frequency $\omega$ and for plan dimension $d$ |
| $d_0$, $\omega_0$ | Lower bounds for plan dimension and frequency, respectively |
| $d_1$, $\omega_1$ | Upper bounds for plan dimension and frequency, respectively |
| $\mathbb{R}_{\geq 0}$ | Set of non-negative real numbers |
| $g$ | Acceleration of free fall ($g \approx 9.81$ m/s$^2$) |
| $(a, b]$ | Half-open interval ($a < x \leq b$) |
| $\tanh^{-1}(\cdot)$ | Inverse hyperbolic tangent function |
| $\ln(\cdot)$ | Natural logarithm |
| $\exp\{\cdot\}$ | Exponential function |

## Abbreviations

| | |
|---|---|
| NPP | Nuclear Power Plant |
| GMI | Ground Motion Incoherence |
| SSI | Soil-Structure Interaction |
| PRA | Probabilistic Risk Assessment |
| PSA | Probabilistic Safety Assessment |
| PSHA | Probabilistic Seismic Hazard Analysis |
| DSA | Deterministic Safety Analysis |
| 1-dof | Single-Degree-of-Freedom |
| GRS | Ground Response Spectrum |
| ISRS | In-Structure Response Spectrum |
| ITF | Incoherence Transfer Function |
| IAEA | International Atomic Energy Agency |
| EPRI | Electric Power Research Institute |
| ASCE | American Society of Civil Engineers |
| SEI | Structural Engineering Institute |
| STUK | Radiation and Nuclear Safety Authority (Säteilyturvakeskus) |

# 1 Introduction

Over the past decades, the field of nuclear safety has evolved drastically with the help of new technologies and a better understanding of risk management. At the Loviisa Nuclear Power Plant (NPP), this has meant that the impact of many traditional hazards, such as equipment faults and fires, have largely been minimized. As a result, the importance of previously overlooked areas—like seismic hazards—has become increasingly prominent. Although rare in the region, large earthquakes have the potential to cause severe equipment damage, which in turn could disrupt critical safety systems and lead to a reactor core meltdown.

Loviisa's seismic risks are assessed using both probabilistic and deterministic methods. Although these methods are irreplaceable in providing a fundamental understanding of the risks that lead to a core meltdown, they typically include simplifying assumptions that produce conservative results.

One such simplification is the common exclusion of the effects of Ground Motion Incoherence (GMI) from seismic load estimations. GMI refers to the spatial variability of seismic ground motion that is caused by differences in wave arrival times, amplitudes, and phases in different parts of the foundations of the structure. This effect is most pronounced at higher frequencies, as the wavelengths of seismic waves get shorter and more susceptible to local variations in soil and structural properties [1]. As reflected in prior research [2, 3, 4, 5], GMI can significantly reduce the seismic forces experienced by the building and its equipment during an earthquake. Despite this, the effect is not systematically included in seismic assessments for the Loviisa NPP, which may lead to overly protective design solutions and unrealistically high demands for existing equipment.

The primary objective of this project is to conduct a comprehensive literature review on the effects of GMI to assess both the necessity and the methodology for integrating it into the context of Loviisa. The study focuses on evaluating whether GMI should be accounted for in seismic hazard and structural response assessments for the site, and if so, identifying the most applicable and justifiable approaches for its inclusion. In addition to the literature review, the project aims to develop and present a computational example that illustrates the effectiveness of the proposed method.

# 2 Background

The realistic evaluation of the seismic performance of NPPs requires a fundamental understanding of its surrounding concepts. This section covers three key areas that form the basis for analyzing GMI: First, it introduces the methodologies used in the seismic safety assessment of NPPs, drawing a clear line between probabilistic and deterministic approaches. Then, it presents the formulation of response spectra, which are used to eventually quantify GMI. Finally, it briefly discusses soil-structure interaction (SSI) through which various types of variability in ground motion can also impact nuclear facilities.

## 2.1 Safety Assessment of Nuclear Power Plants

Assessing the safety of NPPs is essential to ensure plants operate without endangering people or the environment. Historic events, such as the Fukushima 2011 nuclear accident, have shown how catastrophic consequences realized risks of nuclear energy production can have. To ensure that the likelihood of such events is as low as reasonably attainable, robustness of safety assessment methodologies is crucial. To achieve this, two complementary approaches are widely used: Probabilistic Risk Assessment (PRA) and Deterministic Safety Analysis (DSA).

PRA, also known as Probabilistic Safety Assessment (PSA), evaluates the likelihood and consequences of different accident scenarios. It uses fault and event trees to model how initiating events, such as earthquakes, could lead to core damage. The process is divided into three levels: Level 1 estimates core damage frequency, Level 2 evaluates containment performance and radioactive release, and Level 3 considers off-site consequences. Seismic events are often taken into account on Level 1 in the form of Probabilistic Seismic Hazard Assessment (PSHA), which estimates the probability of different levels of ground motion. To ensure reliability, PRA models should be based on best-estimate models that are rigorously validated according to regulatory criteria. [6, 7, 8]

DSA, on the other hand, focuses on assessing how the NPP performs in predefined scenarios of normal operations and accidents. According to the International Atomic Energy Agency (IAEA) [9], the purpose of DSA is to demonstrate that safety functions, such as reactivity control and heat removal, can be maintained under all conditions. Thus, whereas PRA provides a probabilistic understanding of risk, DSA aims to offer a deterministic confirmation of plant robustness against selected design criteria. This is why conservative assumptions are recommended to be used to leave reassuring safety margins within the designs, although best-estimate methods may also be utilized if appropriately justified [9].

## 2.2 Response Spectra

Response spectra are used in seismic analysis to assist in quantifying the safety assessment process. They represent the peak response of idealized single-degree-of-freedom (1-dof) systems subjected to a specific ground motion. By plotting the maximum response—typically acceleration—as a function of natural frequency, response spectra provide a compact and visual way to understand how structures with different dynamic properties react to the same seismic input. This makes them invaluable for evaluating seismic demand across a range of structural configurations.

The computation of response spectra is a systematic process. It begins by acquiring a ground motion time history, as outlined by Shin and Song [10] and illustrated in Figure 1. The data can be gathered either through empirical measurements or numerical simulations and is used as an input to a set of linear 1-dof systems with varying natural frequencies. The peak response of each system is recorded and subsequently plotted against the frequency to create the response spectrum.

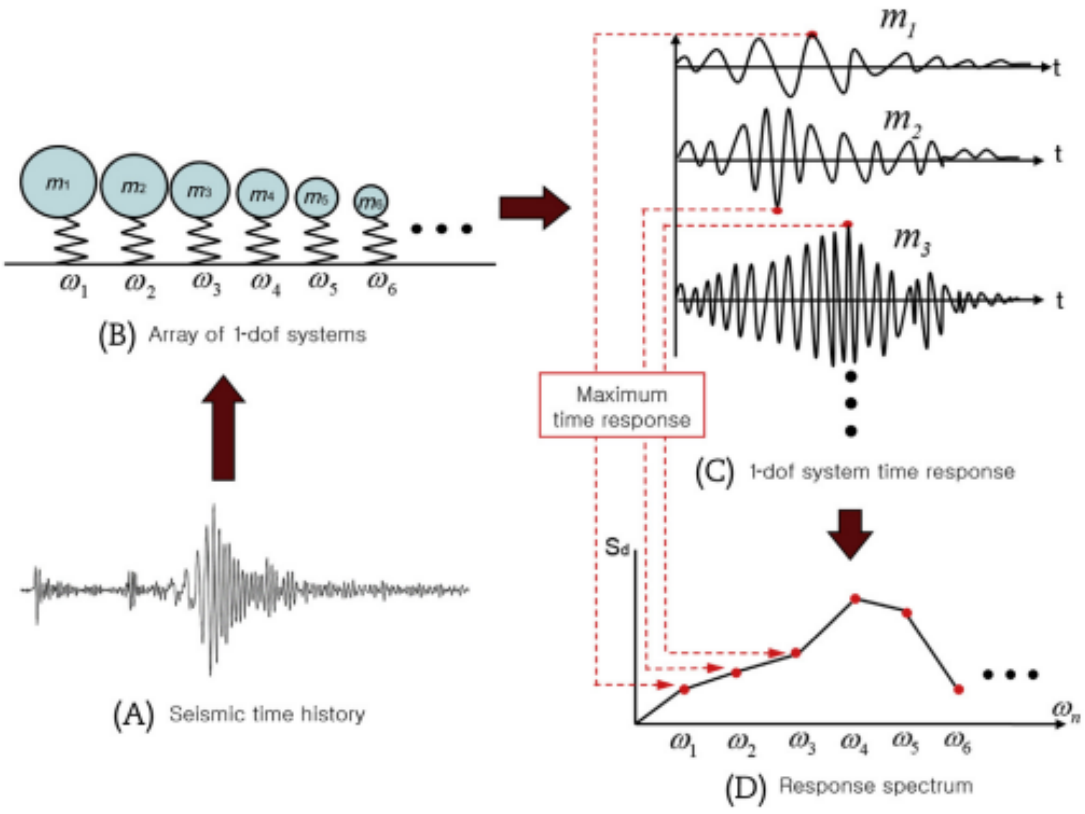


Figure 1: The process of response spectrum computation [10].

Response spectra are classified based on the location of the response measurement. Ground response spectra (GRS) are derived from free-field ground motion and are used to define the seismic input at the base of a structure. In-structure response spectra (ISRS), by contrast, capture the seismic demand at specific points within a structure—typically on floors or walls in the context of NPPs. This distinction is particularly important in nuclear safety assessments, where safety-critical equipment and systems must be evaluated based on the actual seismic environment they experience within the facility. [11]

## 2.3 Soil-Structure Interaction

To correctly formulate the response spectra, the Soil-Structure Interaction (SSI), which refers to the dynamic relation of a structure and its supporting soil, needs to be considered. Unlike the fixed-base assumption, which treats the foundation as rigid, SSI accounts for soil deformation and energy dissipation as seismic waves propagate through the ground. The concept has evolved significantly since the late 19th century, with major advancements driven by the nuclear and offshore industries, the development of finite element methods, and the increasing demand for accurate seismic safety assessments. [12]

Modern SSI analysis utilizes advanced computational tools. According to Islam et al. [13], finite element software such as ABAQUS, ANSYS, and LS-DYNA are widely used for detailed modeling. In contrast, specialized programs like SASSI and CLASSI are preferred in the nuclear industry due to their frequency-domain substructure capabilities. Among these, SASSI is particularly valued for its ability to model flexible volumes and perform substructure subtraction. While these tools are indispensable for modeling soil sites, their integration with related concepts, such as GMI, adds considerable complexity to the analysis [2].

Furthermore, the dynamic response of a structure can vary significantly depending on whether it is founded on flexible soil or hard rock [1]. Generally, the softer the soil, the more pronounced the impact of SSI on the response spectrum. In hard-rock conditions—such as those at the Loviisa NPP—and with coherent seismic input SSI effects are typically so minimal that they can be considered insignificant. In such cases, the structure behaves like a fixed-base system, and GMI becomes the dominant factor influencing seismic response. However, in the presence of incoherence, the effects of SSI become highly site-specific, which is why recent standards mandate the consideration of SSI in all contexts where GMI is relevant [14].

# 3 Ground Motion Incoherence

Ground Motion Incoherence (GMI) captures the spatial variability of seismic ground motion across a structure's foundation. Contrary to the idealized assumption of uniform ground shaking, real-world seismic events often produce motions that vary in both amplitude and phase across different locations of the foundation. This leads to a partial cancellation of seismic inputs and becomes particularly significant at high frequencies (typically above 10 Hz) and for large, rigid structures such as the buildings of NPPs. [1]

## 3.1 Coherency Function

The coherency function is a mapping of frequency and distance that quantifies the degree of similarity between ground motions recorded at two spatially separated locations. It is a fundamental tool for characterizing GMI, as it describes how seismic waves lose correlation over space due to scattering, wave passage effects, and local site conditions [14].

### 3.1.1 Mathematical Formulation

According to the Electric Power Research Institute (EPRI) [15], the coherency function $\gamma_{ij}(\omega)$ between two stations $i$ and $j$ at frequency $\omega$ is defined as

$$\gamma_{ij}(\omega) = \frac{S_{ij}(\omega)}{S_{ii}(\omega)S_{jj}(\omega)}, \tag{1}$$

where $S_{ij}(\omega)$ is smoothed cross-spectrum between stations $i$ and $j$, and $S_{ii}$, $S_{jj}$ are the auto-spectra at the respective stations. Detailed formulations for these spectral components are provided in [15].

In short, the cross-spectral density $S_{ij}(\omega)$ is a complex value that quantifies how much of the frequency component $\omega$ is shared between the two signals at locations $i$ and $j$. A large magnitude of $S_{ij}$ indicates strong correlation at that frequency, while values near zero suggest little to no correlation. In contrast, the auto-spectral density is a real-valued function representing the power of the signal at a given frequency at a single location.

Equation (1) yields a complex-valued coherency, which can be challenging to interpret directly. For practical applications, its absolute value, known as lagged coherency, is commonly used. This measure produces a real number between zero and one that is similar to the correlation coefficients. In addition to its simplicity, lagged coherency has a statistical advantage: its inverse hyperbolic tangent transformation,

$\tanh^{-1}(|\gamma_{ij}(\omega)|)$, is approximately normally distributed. This makes the transformation more suitable for statistical modeling and forms the basis for constructing empirical coherency models, which allow for a more accurate and site-specific simulation of GMI effects. [15]

### 3.1.2 Empirical Coherency Models

Over the last decades, numerous empirical and semi-empirical models have been developed to represent the spatial coherency of ground motion [5]. These models aim to capture how coherency decays with increasing separation distance and frequency, based on observed data from seismic arrays.

One of the most influential and widely used models is Abrahamson's formulation for hard-rock sites [16]. It is an update to the original version presented in [15], which was developed for soil and soft-rock conditions. Mathematically, the updated formulation can be expressed as

$$\gamma_{ij}(\omega, d_{ij}) = \left[1 + \left(\frac{\omega \tanh(a_3 d_{ij})}{a_1 f(d_{ij})}\right)^{n_1(d_{ij})}\right]^{-1/2} \left[1 + \left(\frac{\omega \tanh(a_3 d_{ij})}{a_2}\right)^{n_2}\right]^{-1/2}, \quad (2)$$

where $\omega$ is the frequency, $d_{ij}$ is the separation distance between locations $i$ and $j$, and $a_1$, $a_2$, $a_3$, $n_1(d_{ij})$, $n_2$, $f(d_{ij})$ are empirical coefficients given for horizontal ground motion in Table 1. Coefficients for vertical motion can be found in [16].

Table 1: Abrahamson's empirical coherency function coefficients for horizontal ground motion on hard-rock sites [16].

| **Coefficient** | **Value** |
|---|---|
| $a_1$ | 1.0 |
| $a_2$ | 40 |
| $a_3$ | 0.4 |
| $n_1(d_{ij})$ | $3.80 - 0.040 \cdot \ln(d_{ij} + 1) + 0.0105[\ln(d_{ij} + 1) - 3.6]^2$ |
| $n_2$ | 16.4 |
| $f(d_{ij})$ | $27.9 - 4.82 \cdot \ln(d_{ij} + 1) + 1.24[\ln(d_{ij} + 1) - 3.6]^2$ |

This model is based on data from the Pinyon Flat seismic array, a granite site located in Southern California between the San Jacinto and southern San Andreas Faults [16]. Despite its site-specific origin, Abrahamson et al. [17] have shown that coherency does not significantly depend on site conditions or earthquake magnitude, except for locations with pronounced topographic effects. As a result, the model has been considered applicable to other hard-rock regions, including the Loviisa site, although more recent studies [18, 19] have begun to challenge this conclusion, as discussed further in Section 3.4.

## 3.2 Impact of Soil and Rock Characteristics

As discussed in Section 2.3, the dynamic response of a structure is strongly influenced by the characteristics of the surface on which it is founded. In general, both SSI and GMI significantly affect structures on soil sites, whereas the influence of SSI diminishes for hard-rock sites [1]. According to ASCE/SEI Standard 7-22 [20], site classification is based on the average shear wave velocity $\bar{v}_s$, as shown in Table 2. For consistency, the original velocity units in [20] have been converted from feet per second (ft/s) to meters per second (m/s) and rounded to the nearest 50 units.

Table 2: Site classification based on shear wave velocity [20].

| | **Site Class** | $\bar{v}_s$ **(m/s)** |
|---|---|---|
| A | Hard rock | $(1500, \infty)$ |
| B | Medium hard rock | $(900, 1500]$ |
| BC | Soft rock | $(650, 900]$ |
| C | Very dense sand or hard clay | $(450, 650]$ |
| CD | Dense sand or stiff clay | $(300, 450]$ |
| D | Medium dense sand or stiff clay | $(200, 300]$ |
| DE | Loose sand or medium stiff clay | $(150, 200]$ |
| E | Very loose sand or soft clay | $[0, 150]$ |

Due to the higher propagation speed of seismic waves in hard-rock environments, ground motion tends to remain more coherent at such sites [1]. This is primarily because the variation in arrival times across the foundation is smaller. However, as illustrated in Figure 2, coherency decreases significantly at frequencies above 10 Hz, regardless of the site's classification. This effect becomes more pronounced with increasing separation distance, making it especially relevant for large structures.

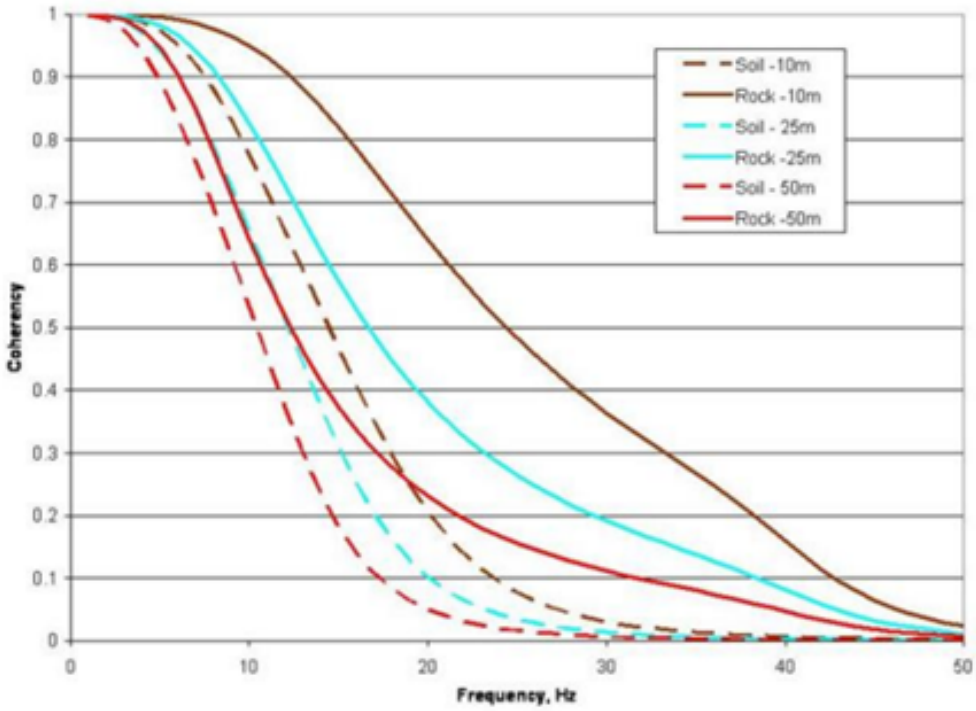


Figure 2: Coherency as a function of frequency for rock and soil sites at different separation distances [1].

Although incoherence is generally lower at rock sites, this does not necessarily imply that GMI is less significant in such settings. Because GMI primarily affects high-frequency components—and because SSI, which also damps high-frequency motion, is generally negligible at rock sites—the relative impact of GMI can be greater in these environments [1, 3]. In other words, while the absolute level of incoherence may be reduced, its influence on structural response becomes more prominent due to the lack of competing damping mechanisms. As a result, accurate modeling of GMI remains essential for seismic analysis and design at hard-rock sites.

## 3.3 Modeling of GMI

Modern models of GMI rely largely on the development of adequate empirical coherency models discussed in Section 3.1.2 and by Zouatine et al. [5]. As their application requires complex computations achievable only with dedicated software, accurate GMI models have existed only for a couple decades [2].

### 3.3.1 Direct Application of GMI in SSI Analysis

Integrating GMI into SSI analysis has become critically important in modern seismic design, particularly for safety-related structures such as NPPs. Recent seismic de-

sign standards, including ASCE/SEI 4-16 [14], explicitly mandate the consideration of SSI effects in all GMI analyses. This requirement reflects a growing recognition of the complex nature of the influence that spatial variability in ground motion can have on structural response.

According to ASCE/SEI 4-16, when GMI is accounted for, SSI analysis must be performed regardless of the stiffness of the supporting soil or rock beneath the foundation. This differs from earlier practices where SSI effects were often neglected for structures founded on very stiff or rock-like materials [14]. The rationale is that even in such cases, incoherent seismic wavefields can alter the characteristics and magnitude of SSI due to the differential motion experienced across the structure's foundation.

GMI is typically included in SSI analysis using coherency functions, which modify the input motion model of the simulation. However, this implementation is far from straightforward. As noted in [14], applying coherency functions is technically complex and requires rigorous verification. This includes ensuring that the numerical models are accurate enough to represent the observed differences in ground motion and that the software can handle the increased computational demands.

A detailed methodology for implementing GMI in SSI analysis is provided by Ostadan and Deng in [21], who integrate spatially variable ground motions into SASSI-based SSI models. Their approach involves modifying the input motion power spectral density matrices with the coherency function to reflect the reduced coherency between different points on the foundation. This produces a more realistic simulation of the seismic input that captures the effects of wave scattering and arrival time differences.

### 3.3.2 Scaling Input Fourier Amplitude

In an attempt to simplify the implementation of GMI, EPRI proposed an alternative approach that utilizes incoherency transfer functions (ITFs) to directly modify response spectra on the Fourier amplitude scale [2]. These functions are fundamentally frequency-dependent scattering matrices derived from empirical coherency functions, such as the one defined in Equation (2), and modified according to the characteristics of the site and the structure. Because of this, ITFs must be developed on a site-specific basis using specialized computational tools like SASSI or CLASSI.

The core concept of the method involves applying the ITF multiplicatively to the Fourier amplitude spectrum of the free-field ground motion. This results in a modified input spectrum that is decreased at frequencies where incoherence is most significant. The ITF is defined as a function of frequency and foundation dimen-

sions, but notably, it is independent of the foundation's geometric shape—at least for rectangular and square foundations. This generality improves its applicability in a wide range of structural configurations. [2]

Although conceptually similar to empirical coherency functions, the mathematical formulation of ITFs is more complex and cannot be achieved with elementary applications. However, once derived, the ITF can be approximated using simplified expressions. For example, in the EPRI study [2], the ITF for a hard-rock site with a 22500-square-foot (2090 $m^2$) foundation was approximated as

$$ITF(\omega) = \left[1 + \left(\frac{\omega \tanh(k_1)}{k_2}\right)^{k_3}\right]^{-k_4},$$

where $\omega$ is the frequency of the ground motion, and $k_1$ through $k_4$ are empirical coefficients listed in Table 3.

Table 3: Coefficients in the approximated ITF [2].

| **Coefficient** | **Horizontal Motion** | **Vertical Motion** |
|---|---|---|
| $k_1$ | 0.006 | 0.04 |
| $k_2$ | 0.08 | 0.5 |
| $k_3$ | 2.4 | 2.5 |
| $k_4$ | 0.75 | 0.5 |

While this method yields results that closely align with those obtained through direct GMI implementation, the computational simplifications it offers are relatively modest, as it still relies on the same specialized software. Nonetheless, from a regulatory perspective, the ITF-based approach is considered a valid and efficient alternative that satisfies the requirements of recent seismic design standards [14].

### 3.3.3 Base Slab Averaging

Recent standards also permit considering incoherence through the application of base slab averaging [20]. This method, formally classified under SSI, refers to a kinematic interaction effect that is conceptually identical to GMI and occurs when the foundation of a structure is sufficiently stiff relative to the vertical lateral force-resisting elements and the underlying soil. Under such conditions, the foundation acts as a spatial filter, averaging out high-frequency components of the seismic input across its footprint. [20]

Unlike dynamic interaction effects—such as foundation damping—which depend on the dynamic properties of the soil-structure system, base slab averaging is dictated exclusively by the size and stiffness of the foundation and the spatial characteristics

of the incoming seismic wavefield. This distinction is important, as it allows base slab averaging to be treated independently of soil nonlinearity or structural flexibility. [22]

To quantify this effect, the ASCE/SEI 7-22 standard [20] introduces a modification factor, denoted $RRSB_{sa}$, which is applied to the response spectrum to account for the reduction in seismic demand. The factor is calculated using the expression

$$RRSB_{sa} = 0.25 + 0.75 \cdot \left[ \frac{1}{b_0^2} (1 - \exp\{-2b_0^2\} \cdot B_{bsa}) \right]^{1/2}, \tag{3}$$

where

$$B_{bsa} = \begin{cases} 1 + b_0^2 + b_0^4 + \frac{b_0^6}{2} + \frac{b_0^8}{4} + \frac{b_0^{10}}{12}, & \text{for } b_0 \leq 1 \\ \exp\{2b_0^2\} \cdot \left[ \frac{1}{\sqrt{\pi} b_0} \left( 1 - \frac{1}{16 b_0^2} \right) \right], & \text{for } b_0 > 1 \end{cases},$$

$$b_0 = 0.0023 \cdot \left( \frac{b_e}{T} \right),$$

where $b_e$ is the effective foundation size in meters and $T$ is the spectral period of interest. The procedure for computing $b_e$ is detailed in the standard [20].

This formulation assumes that the foundation system includes structural mats or interconnected elements (e.g., grade beams) that provide sufficient lateral stiffness to enable spatial filtering [20]. However, ASCE/SEI 7-22 specifies that this method is only formally applicable to structures located on Site Classes C through E, as defined in Table 2 in Section 3.2. While this does not explicitly prohibit the use of base slab averaging at rock sites, it means that Equation (3) has not been validated for such conditions. Consequently, its application in those contexts should be approached with caution and supported by additional justification and site-specific studies.

### 3.3.4 Response Spectra Reduction Factors

Before the widespread availability of advanced computational tools capable of modeling spatially variable ground motions, engineers relied on simplified methods to account for the effects of GMI. One such method, featured in the now-outdated ASCE 4-98 standard [23], involved using response spectra reduction factors, which provided a conservative, but practical way of incorporating GMI effects into seismic design and analysis.

The rationale behind this approach stems from the recognition that traditional SSI analyses, based on vertically propagating and coherent seismic waves, tend to overestimate in-structure responses. In the absence of detailed incoherency modeling, it

was considered conservative to apply reductions directly to the GRS to approximate the filtering effects of GMI. [23]

Like ITFs, these reduction factors depend on frequency and foundation plan dimensions. To account for the increase in incoherence for large structures and high frequencies, the relative spectral reductions grow with plan dimensions and frequencies. For example, as shown in Table 4, a foundation with a plan dimension of 45 m (150 ft) experiences no reduction at 5 Hz, a 10% reduction at 10 Hz, and a 20% reduction at 25 Hz and above. For a larger foundation of 90 m (300 ft), the reductions are more substantial: 20% at 10 Hz and 40% at 25 Hz and above. Here, the plan dimension refers to the side length of a square foundation. However, as demonstrated in [2], the effects of incoherence are equivalent for square and rectangular foundations with the same area. Accordingly, for rectangular foundations, the referenced plan dimension corresponds to the side length of a square with an equivalent area.

Table 4: Spectral reduction factors for different frequencies and plan dimensions [23].

| **Frequency (Hz)** | **Reduction Factor for Plan Dimension of** | |
|---|---|---|
| | 45 m (150 ft) | 90 m (300 ft) |
| $\leq 5$ | 1.0 | 1.0 |
| 10 | 0.9 | 0.8 |
| $\geq 25$ | 0.8 | 0.6 |

For structures with plan dimensions other than those listed, ASCE 4-98 suggests using linear interpolation or extrapolation to estimate appropriate reduction factors. Similarly, for intermediate frequencies, interpolation in the ln-ln plane has been adopted in previous implementations [24]. Mathematically, linear interpolation and extrapolation with respect to the plan dimensions can be expressed as

$$r(\omega, d) = r(\omega, d_0) + (d - d_0)\frac{r(\omega, d_1) - r(\omega, d_0)}{d_1 - d_0}, \text{ for } \omega, d \in \mathbb{R}_{\geq 0}, \tag{4}$$

where $r(\omega, d)$ is the reduction factor at frequency $\omega$ for foundation plan $d$, $d_0$ and $d_1$ are the lower and upper bounds of the specified plan dimension interval (45–90 m). When $d_0 \leq d \leq d_1$, the formula corresponds to interpolation; otherwise, it represents extrapolation.

Similarly, interpolation in the ln-ln plane for intermediate frequencies between 5–10 Hz or 10–25 Hz is given by

$$\ln(r(\omega, d)) = \ln(r(\omega_0)) + [\ln(\omega) - \ln(\omega_0)]\frac{\ln(r(\omega_1, d)) - \ln(r(\omega_0, d))}{\ln(\omega_1) - \ln(\omega_0)}, \quad \text{for } \omega_0 \leq \omega \leq \omega_1, d \in \mathbb{R}_{\geq 0} \tag{5}$$

In the ASCE 4-98 standard [23], spectral reduction factors are considered applicable across a range of damping values and are recommended for use with both horizontal and vertical response spectra. Although more recent standards—such as ASCE/SEI 4-16 [14], as discussed in Section 3.3.1—prohibit the use of such simplified methods for GMI modeling, they may still serve a valuable role in preliminary design or assessments where full incoherency modeling is not feasible.

However, according to Chen et al. [3], it is important to note that the effectiveness of these factors depends heavily on the shape of the free-field ground response spectrum and must also consider induced rotational effects on the structure. Thereby, to be assured that the factors remain as a conservative estimate, one should already have a fairly certain estimate on the magnitude of the GMI effects on the structure of interest through prior research or studies from comparable regions.

## 3.4 GMI in Prior Research

The effects of GMI have been extensively researched for a variety of large-scale structures, such as bridges, dams, and nuclear power plants. The results of these studies have been rigorously documented in numerous technical reports [2, 15, 21, 24], conference proceedings [3, 4, 5, 18], and peer-reviewed journal articles [25, 26, 27, 28, 19]. While notable methodological and contextual differences exist, a common conclusion is clear: GMI can significantly influence seismic demand, particularly in the high-frequency range.

Prior research consistently shows that when the dominant spectral acceleration of ground motion occurs at frequencies above 10 Hz, GMI can reduce the spectral peaks at those frequencies by more than 50%. On the other hand, when seismic energy is concentrated at lower frequencies, the dynamic interaction between GMI and SSI effects can sometimes even lead to an increase in these peaks [28]. This is especially true when the incoherent input excites structural modes that are otherwise less responsive under coherent motion.

Although these findings are informative, much of the existing research has focused on specific case studies using advanced numerical modeling tools. These studies often emphasize the application of GMI in complex SSI simulations but give limited attention to the validation of the models themselves. As a result, the findings and methods are not always generalizable without site-specific calibration.

Some researchers have also raised concerns about using generic coherency models—such as Abrahamson's models—at sites with geologic or topographic conditions that differ significantly from those used to develop the original models. For example, Dan et al. [18] and Lee et al. [19] questioned the applicability of such models in non-

standard settings and highlighted the need for caution when applying them without local validation. Lee et al. found that Abrahamson's hard rock model (Equation (2)) may overestimate incoherency at sites with significantly higher $\bar{v}_s$ than the Pinyon Flat site ($\bar{v}_s = 1030$ m/s), particularly at separation distances below 50 meters and frequencies above 25 Hz. The authors argue that this is caused by a stronger correlation between shear wave velocity and coherence at short separation distances than was previously assumed.

Importantly, the effects of GMI are not easily quantified without detailed knowledge of the site conditions and structural configuration. To accurately capture the full range of potential responses, incoherence should therefore be explicitly incorporated into the response spectrum computation process. While conservatively simplified methods—such as response spectra reduction factors—have been previously proposed, their use in research has been limited. This is likely because, at the time these methods were introduced, both the understanding of GMI and the computational tools required for accurate modeling were still in early stages. Consequently, many early studies neglected the effect altogether. However, as computational capabilities and theoretical understanding have advanced, more sophisticated and site-specific modeling approaches have become the norm in contemporary research.

# 4 Discussion and Computational Example

## 4.1 Recommendation for the Modeling of GMI for Loviisa NPP

Based on existing literature and engineering standards, it is evident that GMI is a complex phenomenon that has a high importance for sites where high-frequency spectral accelerations dominate the seismic hazard. This is precisely the case at the Loviisa NPP, where the structures are founded directly on the exceptionally hard bedrock ($\bar{v}_s = 3200$ m/s) and the most significant spectral content occurs at frequencies above 10 Hz [29]. Furthermore, some coherent in-structure response spectra for the site [30] predict significant accelerations at frequencies approaching 100 Hz which are likely overestimated due to the exclusion of GMI.

As noted in previous sections, the complexity of modeling the spatially incoherent seismic wave field means that simplified models for estimating GMI effects are not permitted unless properly justified. This reflects the broader consensus that the effects of incoherence are highly site- and structure-specific and, therefore, cannot be reliably captured through generic approximations. Consequently, the exact magnitude and nature of GMI effects cannot be known with certainty without detailed modeling. For this reason, it is generally recommended that GMI ought to be integrated directly into SSI analysis using specialized software capable of handling spatially variable input motions and site-specific coherency functions.

The research context at the Loviisa site, however, presents a unique challenge. While previous studies [29] employing Abrahamson's hard rock model within the CLASSI software framework have shown that GMI can significantly reduce high-frequency structural responses for some buildings at the site, current models for other structures have not been implemented in this software. This limitation necessitates a pragmatic approach. Nonetheless, the earlier findings underscore the importance of GMI at Loviisa—even if Abrahamson's model may overestimate incoherence for smaller structures at frequencies above 25 Hz, given the site's exceptionally hard bedrock [19].

Considering the well-established characteristics of the Loviisa site—namely, its hard-rock foundation, high-frequency spectral content, and prior evidence of substantial GMI-induced reductions—it is reasonable to conclude that unmodified, coherent response spectra are overly conservative, even for deterministic analyses. In this context, applying simplified response spectrum reduction factors offers a practical alternative that has the potential to mitigate this excessive conservatism. However, the broader applicability of these factors to buildings with varying configurations and dimensions remains uncertain and warrants further investigation.

In the context of PRA, on the other hand, where the objective is to quantify best-estimate structural responses, the integration of GMI into SSI analysis becomes even more critical. Ideally, this would be done using advanced modeling tools and site-specific coherency functions. Nonetheless, in the absence of such resources, applying reduction factors to unmodified GRS remains the preferable option.

## 4.2 Computational Example of the Use of Reduction Factors

This section presents a computational example that illustrates the application of spectral reduction factors, as described in Section 3.3.4, to two representative structures with rectangular foundations measuring $30 \times 15$ m and $180 \times 55$ m. The plan dimensions of an area-equivalent square foundations are 21.2 m and 99.5 m, respectively. The reduction factors are applied to a sample GRS taken from the 2013 Radiation and Nuclear Safety Authority (STUK) guide YVL B.7 [31], which has been scaled to the peak ground acceleration of $0.1g$ as instructed in the guide. This spectrum is considered to reasonably closely match the characteristics of the Loviisa site.

The appropriate reduction factors are determined by interpolating the values from Table 4 based on the structure's plan dimension. The interpolation follows the procedure defined in Equation (4). Since the example spectrum consists of discrete frequency points, none of which fall within the 5–10 Hz or 10–25 Hz ranges, no interpolation across frequency bands is necessary. The resulting reduction factors used in the computation are summarized in Table 5.

Table 5: Spectral reduction factors used in the example computation.

| **Frequency (Hz)** | **Reduction Factor for Plan Dimension of** | |
|---|---|---|
| | 21.2 m | 99.5 m |
| $\leq 5$ | 1.0 | 1.0 |
| 10 | 0.95 | 0.78 |
| $\geq 25$ | 0.91 | 0.56 |

To obtain the incoherent spectrum, each point of the original GRS is multiplied by the corresponding reduction factor, effectively scaling down the spectrum at frequencies above 10 Hz. As shown in Figure 3, the resulting reductions are highly sensitive to the size of the structure.

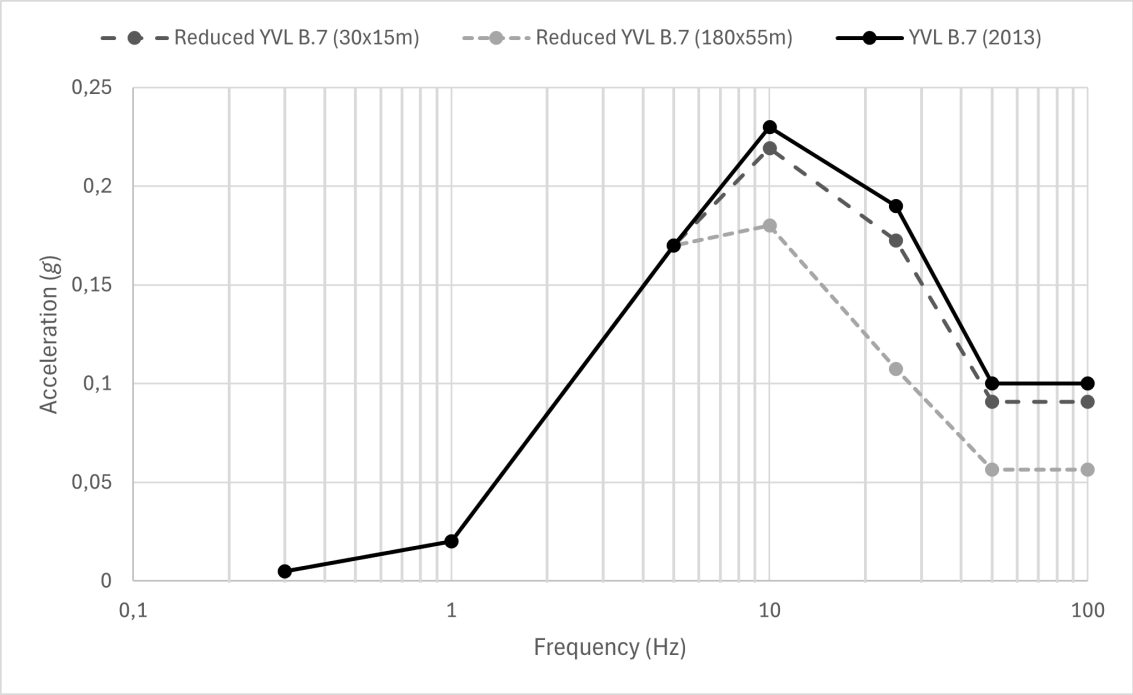


Figure 3: Effect of spectral reduction factors to STUK YLV B.7 example GRS on two differently-sized structures.

Based on Table 5 and Figure 3, it is evident that the spectral reduction is significantly greater for structures with larger foundation footprints. Although previous studies [2, 4, 25] have reported incoherence effects leading to response reductions exceeding 50% for large buildings, this study alone cannot confirm that the simple reduction factors remain conservative when scaled according to the ASCE 4-98 standard [23] guidelines. On the other hand, for small structures, the reduction factors may still be overly conservative to provide notable improvements. Thus, to apply these factors to the structures of the Loviisa site, future research should explore alternative scaling methods to ensure that an appropriate level of conservatism is maintained for all buildings.

# 5 Conclusion

This project has examined the effects of ground motion incoherence in the context of nuclear power plants, with a specific focus on the Loviisa NPP. Through a comprehensive literature review, it has been demonstrated that GMI can significantly influence structural response, especially in high-frequency seismic environments typical for hard-rock sites like Loviisa.

The findings suggest that neglecting GMI in hard-rock regions can result in unrealistically conservative demands. However, quantifying this effect has proven to be highly complex, requiring specialized software and site-specific coherency models, which are not always available or are difficult to develop.

Given that there is sufficient prior knowledge of GMI effects at the site of interest, it is concluded that the use of response spectrum reduction factors can serve as a potential alternative if more advanced techniques cannot be utilized. However—as reflected in the computational example presented in this study—these factors may not be as conservative as previously thought, especially for large buildings. Thus, additional research is required to draw definitive conclusions regarding their applicability.

Nonetheless, the findings support the integration of GMI in both probabilistic and deterministic seismic assessments at the Loviisa NPP. Where full incoherency modeling is not feasible, simplified methods—appropriately justified and conservatively applied—may still offer meaningful improvements over previous, fully coherent analyses. However, future work should aim to assess the appropriate intensity of scaling the reduction factors and to explore whether slightly more sophisticated, yet computationally reasonable, alternatives can be developed to enhance accuracy without compromising practicality.

# References


[1] Electric Power Research Institute (EPRI). Seismic Fragility and Seismic Margin Guidance for Seismic Probabilistic Risk Assessments. Technical report, Palo Alto, CA, September, 2018. 3002012994.

[2] Electric Power Research Institute (EPRI). Effect of Seismic Wave Incoherence on Foundation and Building Response. Technical report, Palo Alto, CA, December, 2005. 1012966.

[3] R. Chen et al. Seismic Analysis for a Reactor Building with High Frequency Ground Motion. In *Proceedings of the 20th International Conference on Structural Mechanics in Reactor Technology (SMiRT 20)*, Espoo, Finland, August 9–14, 2009.

[4] A. Nour, A. Cherfaoui, V. Gocevski, and P. Léger. CANDU 6 Nuclear Power Plant: Reactor building floor response spectra considering seismic wave incoherency. In *Proceedings of the 15th World Conference on Earthquake Engineering*, Lisbon, Portugal, September 24–28, 2012.

[5] M. Zouatine et al. Investigating the Impact of Spatial Variation of Seismic Ground Motions on Reactor Containment Building Response. In *Proceedings of the 27th International Conference on Structural Mechanics in Reactor Technology*, Yokohama, Japan, March 3–8, 2024.

[6] C. Smith. Chapter 1 - Introduction. In C. Smith, K. Blanc, and D. Mandelli, editors, *Risk-informed Methods and Applications in Nuclear and Energy Engineering*, pages 1–12. Academic Press, 2024.

[7] International Atomic Energy Agency (IAEA). Development and Application of Level 1 Probabilistic Safety Assessment for Nuclear Power Plants. Technical report, Vienna, Austria, 2024. No. SSG-3 (Rev. 1).

[8] J. Baker. Introduction to Probabilistic Seismic Hazard Analysis, 2015. *White Paper Version 2.1.*

[9] International Atomic Energy Agency (IAEA). *Deterministic Safety Analysis for Nuclear Power Plants.* Vienna, Austria, 2019. No. SSG-2 (Rev. 1).

[10] G. Shin and O. Song. A Time-Domain Method to Generate Artificial Time History from a Given Reference Response Spectrum. *Nuclear Engineering and Technology*, 48(3):831–839, 2016.

[11] L. Bo. *Response Spectra for Seismic Analysis and Design.* Phd dissertation, University of Waterloo, Ontario, Canada, 2015.

[12] L. Menglin, W. Huaifeng, and C. Y. Z. Xi. Structure–soil–structure interaction: Literature review. *Soil Dynamics and Earthquake Engineering*, 31(12):1724–1731, 2011.

[13] M. R. Islam et al. Seismic soil-structure interaction in nuclear power plants: an extensive review. *Results in Engineering*, 23(5):102694, 2024.

[14] American Society of Civil Engineers (ASCE). *Seismic Analysis of Safety-Related Nuclear Structures*. 2017. ASCE/SEI Standard 4-16.

[15] Electric Power Research Institute (EPRI). Program on Technology Innovation: Spatial Coherency Models for Soil-Structure Interaction. Technical report, Palo Alto, CA, January, 2006. 1012968.

[16] N. A. Abrahamson. Hard-Rock Coherency Functions Based on the Pinyon Flat Array Data, July, 2007. Draft report to EPRI.

[17] N. A. Abrahamson, J. F. Schneider, and J. C. Stepp. The spatial variation of earthquake ground motion and effect of local site conditions. In *Proceedings of the Tenth World Conference Earthquake Engineering*, Madrid, Spain, July 19–24, 1992.

[18] M. Dan, J. Youngsun, and L. Inhee. Understanding seismic motion incoherency modeling and effects on SSI and SSSI responses of nuclear structures. In *Proceedings of the 24th Conference on Structural Mechanics in Reactor Technology (SMiRT)*, Busan, Korea, August 20–25, 2017.

[19] Y. Lee et al. Spatial coherency analysis of seismic motions from a hard rock site dense array in Busan, Korea. *Bulletin of Earthquake Engineering*, 22:7235–7259, 2024.

[20] American Society of Civil Engineers (ASCE). *Minimum Design Loads and Associated Criteria for Buildings and Other Structures*. 2022. ASCE/SEI Standard 7-22.

[21] F. Ostadan and N. Deng. SASSI-SRSS Approach for SSI Analysis with Incoherent Ground Motions. Technical report, Bechtel National, San Francisco, CA, August, 2007.

[22] Applied Technology Council (ATC). A Practical Guide to Soil-Structure Interaction. Technical report, Federal Emergency Management Agency (FEMA), Washington, D.C., December, 2020. FEMA P-2091.

[23] American Society of Civil Engineers (ASCE). *Seismic Analysis of Safety-Related Nuclear Structures and Commentary*. 2000. ASCE Standard 4-98.

[24] Electric Power Research Institute (EPRI). A Methodology for Assessment of Nuclear Power Plant Seismic Margin (Revision 1). Technical report, Palo Alto, CA, August, 1991. NP-6041-SLR1.

[25] W. S. Tseng, K. Lilhanand, D. Hamasaki, J. A. Garcia, and R. Srinivasan. Seismic soil-structure interaction with consideration of spatial incoherence of seismic ground motions: A case study. *Nuclear Engineering and Design*, 269:200–206, 2014.

[26] M. Davoodii, M. K. Jafari, and S. M. A. Sadrolddini. Effect of multi support excitation on seismic response of embankment dams. *International Journal of Civil Engineering*, 11(1):19–29, 2013.

[27] J. H. Lee. Earthquake response analysis of nuclear facilities subjected to incoherent seismic waves based on the random-vibration-theory methodology. *Soil Dynamics and Earthquake Engineering*, 164:107527, 2023.

[28] V. A. Salunkhe, R. S. Jangid, and R. Ranjan. Potentiality of using seismic motion incoherency in analyzing base isolated reactor building of Indian nuclear power plant: A case study. *Nuclear Engineering and Design*, 432:113829, 2025.

[29] J. M. Jimenez-Chong. Seismic Response Analysis of the Turbine and Control Building for S1 Seismic Input. Technical report, Simpson Gumpertz & Heger, Boston, MA, 2023. LO1-K230-00020.

[30] T. Leppänen. Loviisa 2, Response spectra for the diesel building 2D272, Sections between lines 10 and 14, Results. Technical report, Fortum Power and Heat Oy, Espoo, Finland, 2024. LO2-K272-00004.

[31] Radiation and Nuclear Safety Authority (STUK). YVL B.7: Provisions for Internal and External Hazards at a Nuclear Facility, 2013.